

## Screw Dislocations in Chiral Magnets

Maria Azhar<sup>1</sup>, Volodymyr P. Kravchuk<sup>1,2</sup> and Markus Garst<sup>1,3</sup><sup>1</sup>*Institut für Theoretische Festkörperphysik, Karlsruhe Institute of Technology, 76131 Karlsruhe, Germany*<sup>2</sup>*Bogolyubov Institute for Theoretical Physics of National Academy of Sciences of Ukraine, 03143 Kyiv, Ukraine*<sup>3</sup>*Institute for Quantum Materials and Technology, Karlsruhe Institute of Technology, 76131 Karlsruhe, Germany*
 (Received 22 September 2021; revised 23 December 2021; accepted 28 February 2022; published 12 April 2022)

Helimagnets realize an effective lamellar ordering that supports disclination and dislocation defects. Here, we investigate the micromagnetic structure of screw dislocation lines in cubic chiral magnets using analytical and numerical methods. The far field of these dislocations is universal and classified by an integer strength  $\nu$  that quantifies its Burgers vector. We demonstrate that a rich variety of dislocation-core structures can be realized even for the same strength  $\nu$ . In particular, the magnetization at the core can be either smooth or singular. We present a specific example with  $\nu = 1$  for which the core is composed of a chain of singular Bloch points. In general, screw dislocations carry a noninteger but finite skyrmion charge so that they can be efficiently manipulated by spin currents and should contribute to the topological Hall effect.

DOI: 10.1103/PhysRevLett.128.157204

**Introduction.**—The Dzyaloshinskii-Moriya interaction (DMI) in cubic chiral magnets like MnSi, FeGe, or Cu<sub>2</sub>OSeO<sub>3</sub> favors helimagnetic long-range order in a large region of the phase diagram [1–7]. A finite field  $\mathbf{H}$  aligns the helix axis and, in addition, tilts the magnetic moments towards the field direction giving rise to a conical magnetic helix, see Fig. 1(a). This helimagnetic ordering realizes a one-dimensional periodic texture that shares many similarities with other emerging lamellar structures found, e.g., in various soft matter systems [8–10].

In particular, in the limit of weak spin-orbit coupling (SOC) the phase transition from the paramagnetic to the helimagnetic phase at  $\mathbf{H} = 0$  is a fluctuation-driven first-order transition similar to the ones in certain cholesteric liquid crystals or diblock copolymers [11–13]. The correlation length above the critical temperature  $T_c$  possesses a temperature dependence that is well described by weak crystallization theory [14]. This indicates that the paramagnetic regime just above  $T_c$  is characterized by strong correlations that are maintained by the large density of states of paramagnons [15]. It is still an important open issue whether these pronounced magnetic correlations are also at the origin of the non-Fermi liquid behavior observed in MnSi and FeGe upon suppressing the critical temperature towards zero with pressure [16–20].

In this context, the question arises as to whether this intriguing paramagnetic-helimagnetic phase transition can also be understood from the dual perspective as a defect-mediated melting transition [21–23]. A prerequisite to address this question is an understanding of the elementary defects of helimagnetic order. It is well known that defects of lamellar structures in general consist of disclinations and dislocations, which are line defects in case the lamellae are

embedded in three-dimensional space [8]. For helimagnets, such defects were discussed on a phenomenological level by Kléman [24]. Recently, it was shown both theoretically and experimentally that domain walls of helimagnetic order might consist of an arrangement of disclinations and edge dislocations [25–27] very similar to domain walls in cholesteric liquid crystals [28]. Moreover, at helimagnetic twist grain boundaries screw dislocations are expected to

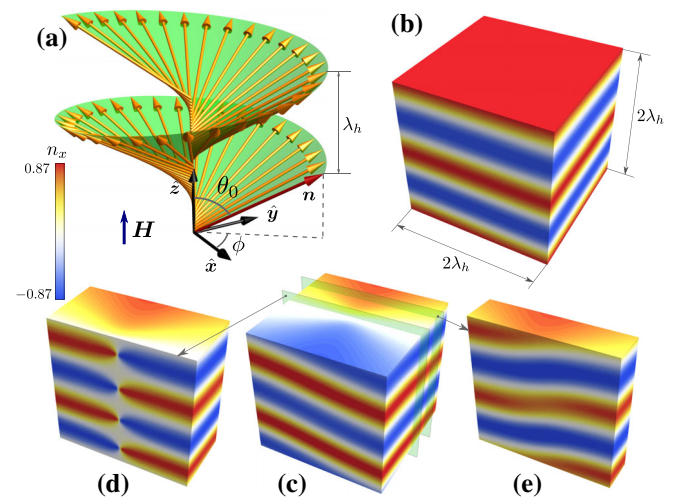


FIG. 1. (a) Conical magnetic helix with pitch  $\lambda_h$  and cone angle  $\theta_0$  enclosed by the magnetic moments and the direction of the applied magnetic field  $\mathbf{H}$ . (b) Helimagnetic order is characterized by equidistant isosurfaces, the hallmark of lamellar order, where, e.g., the  $x$  component of magnetization,  $n_x$ , assumes a particular value. (c)–(e) Example of a screw dislocation with strength  $\nu = 1$  illustrated by different vertical cross sections. The core of this specific example contains a chain of magnetic Bloch points.

occur [8,29]. It was also demonstrated that the motion of edge dislocations is an important relaxation process for disordered helimagnets possibly accounting for the large relaxation times observed experimentally [30–33].

However, there exist additional line excitations within the conical helix phase that are distinct from dislocations and disclinations. In particular, chiral magnets are famously known to host skyrmions, i.e., topological two-dimensional magnetic textures [34]. In bulk magnets, the skyrmion textures extend along the third direction forming skyrmion strings that either condense into a lattice or exist as metastable excitations of the field-polarized phase [7,35,36]; for a recent review see Ref. [37]. It has been demonstrated in Refs. [38,39] that such metastable skyrmion configurations also persist within the conical helix phase upon decreasing the magnetic field below the critical field  $H_{c2}$ . Such skyrmion strings attract each other and can form clusters or even networks [40–42]. Nevertheless, these skyrmion strings within the conical helix phase possess an exponentially decaying far field and, in contrast to dislocation lines, are characterized by a vanishing Burgers vector. In addition, the conical helix can also support localized large-amplitude excitations like bound pairs of hedgehog defects, i.e., Bloch points [43] and even Hopfions [44].

In the present work, we theoretically investigate in detail screw dislocations in cubic chiral magnets. The helimagnetic order defines equally spaced isosurfaces where, e.g., the  $x$  component of the magnetization assumes the same value, see Fig. 1(b). The deviation of isosurfaces from their equilibrium configuration is described by the displacement field  $\mathbf{u}$  [45]. The integral along a loop enclosing a dislocation line,  $\oint d\mathbf{u} = \mathbf{b}$ , is finite and given by the Burgers vector  $\mathbf{b}$  indicating that  $\mathbf{u}$  is singular at the dislocation core. For a screw dislocation,  $\mathbf{b} = \lambda_h \nu \hat{\mathbf{z}}$  is aligned with the helix axis  $\hat{\mathbf{z}}$  and its size is an integer multiple of the helix pitch  $\lambda_h$ , where  $\nu \in \mathbb{Z} \setminus \{0\}$  characterizes the strength of the screw dislocation (sd $_\nu$ ).

Using analytical arguments and numerical simulations we determine the micromagnetic structure of screw dislocations. In the limit of small SOC, when the influence of magnetocrystalline anisotropies is negligible, we find that they possess in the far field the expected universal form of lamellar structures with a displacement vector  $\mathbf{u} = u_z(x, y)\hat{\mathbf{z}}$  where [8–10]

$$u_z(x, y) = \frac{\lambda_h}{2\pi} \nu \chi. \quad (1)$$

Here,  $\chi$  is the polar angle of cylindrical real-space coordinates  $(\rho, \chi, z)$ . Moreover, we show that the magnetization texture at the core of screw dislocations can either be smooth or might contain Bloch points, which we illustrate explicitly for screw dislocations with  $|\nu| = 1$ .

*Theory of cubic chiral magnets.*—The magnetic energy functional  $E = \int d\mathbf{r} \mathcal{E}$  of cubic chiral magnets possesses a density that reads in leading order in SOC

$$\mathcal{E} = A(\partial_i \mathbf{n})^2 + D\mathbf{n}(\nabla \times \mathbf{n}) - M_s \mu_0 H n_z. \quad (2)$$

Here,  $\mathbf{n}$  is a unit vector specifying the orientation of the local magnetization and the magnetic field is applied in the  $z$  direction,  $\mathbf{H} = H\hat{\mathbf{z}}$ ;  $A$  is the exchange constant,  $D > 0$  is the DMI assuming a right-handed chiral magnetic system,  $M_s$  is the saturation magnetization and  $\mu_0$  is the vacuum permeability. Importantly, for zero field  $H = 0$  this density is isotropic with respect to a combined rotation of spin and real space. This rotational symmetry is explicitly broken by magnetocrystalline anisotropies that are, however, weak in the limit of small SOC and will be mostly neglected in the following. We also neglect for simplicity the magnetic dipolar interaction.

It is convenient to consider the representation of  $\mathbf{n} = (\sin \theta \cos \phi, \sin \theta \sin \phi, \cos \theta)$  in terms of polar angle  $\theta$  and azimuthal angle  $\phi$ . For large fields  $H > H_{c2} = D^2/(2A\mu_0 M_s)$  the ground state of Eq. (2) is field polarized with  $\theta = 0$ . The ground state for small fields  $0 \leq H < H_{c2}$  is the conical helix with a position dependent polar angle  $\phi = 2\pi z/\lambda_h$  where the helix pitch  $\lambda_h = 4\pi A/D$ , and the cone angle  $\theta = \theta_0$  with  $\cos \theta_0 = H/H_{c2}$ .

*Far field of screw dislocations.*—Performing an asymptotic analysis of the Euler-Lagrange equations of Eq. (2), for details see the Supplemental Material [46], we find that the conical helix supports screw dislocations with an asymptotic behavior for large distances from their core  $\rho \rightarrow \infty$ ,

$$\theta = \theta_0 + \frac{2\nu \sin^2 \theta_0}{1 + \sin^2 \theta_0} \frac{\lambda_h}{2\pi\rho} \sin \left[ (\nu - 1)\chi + \frac{2\pi z}{\lambda_h} \right] + \mathcal{O}(\rho^{-2}), \quad (3)$$

$$\phi = \frac{2\pi}{\lambda_h} [z + u_z(x, y)] + \mathcal{O}(\rho^{-2}), \quad (4)$$

where  $u_z$  is the universal displacement field of Eq. (1). The dependence of  $\phi$  indicates that the  $(x, y)$  components of the magnetization form a vortex within each plane perpendicular to the applied field, i.e., for each value of  $z$ , and the winding number is just given by the disclination strength  $\nu$ . The structure of the vortex changes from plane to plane as a function of  $z$  due to the linear dependence of  $\phi$  on  $z$ , see Fig. 1.

The far-field configuration allows to determine the topological skyrmion charge for a screw dislocation within each  $z$  plane,  $N_{\text{top}}(z) = \int dx dy \rho_{\text{top}}$ , where  $\rho_{\text{top}} = (1/4\pi)\mathbf{n}(\partial_x \mathbf{n} \times \partial_y \mathbf{n})$ . Note that, in contrast to skyrmions, here  $N_{\text{top}}(z)$  is not an integer. At infinity  $\rho \rightarrow \infty$ , the magnetization  $\mathbf{n}$  has a fixed polar angle  $\theta_0$  and encircles the  $\hat{\mathbf{z}}$  axis  $\nu$  times as a function of real-space angle  $\chi$ . Assuming that the magnetization texture is smooth in a given  $z$  plane, we obtain for the charge

$$N_{\text{top}}(z) = \frac{\nu}{2}(1 - h) + n(z), \quad (5)$$

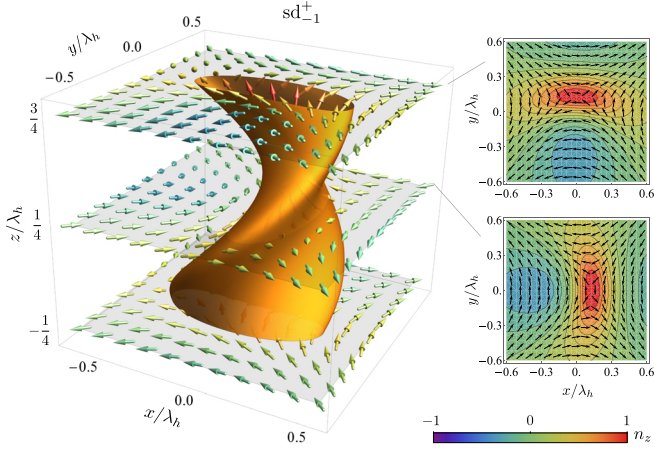


FIG. 2. Core of the screw dislocation  $sd_1^+$  with strength  $\nu = -1$  obtained by micromagnetic simulations for  $H = 0$ . The magnetic moments represented by arrows form within a given  $z$  plane an anti-vortex-like structure. The orange isosurface in the main panel is defined by  $n_z = 1/2$ . The magnetization at the core is preferentially pointing in  $\hat{z}$  direction; the configuration with opposite core magnetization,  $sd_{-1}^-$ , is degenerate at  $H = 0$  (not shown). Note that the periodicity of the core structure along  $z$  is characterized by a wavelength  $2\lambda_h$ .

with the reduced field  $h = H/H_{c2}$ , and  $n(z) \in \mathbb{Z}$  is an integer that depends on the magnetization at the core of the screw dislocation. As we will see below, in case that  $n(z)$  varies with  $z$  the core is singular and contains Bloch points.

Plugging the asymptotics of Eqs. (3) and (4) into Eq. (2) we obtain for the energy of a screw dislocation line per length

$$\varepsilon_{sd} = \varepsilon_{sd}^{\text{core}} + A(2\pi\nu)^2 \frac{h^2(1-h^2)}{2-h^2} \log \frac{R}{\rho_{\text{core}}}, \quad (6)$$

where  $h = H/H_{c2}$ . The length scale  $R$  specifies the extension of the system in radial direction, and  $\rho_{\text{core}}$  is the linear size of the dislocation core with the associated core energy  $\varepsilon_{sd}^{\text{core}}$ . The far-field tail of the screw dislocation gives rise to a contribution to the energy that in general diverges logarithmically with the radial system size  $R$ . This logarithmic contribution vanishes at the transition  $H = H_{c2}$  to the field-polarized phase because the dislocation ceases to be defined when the cone angle vanishes,  $\theta_0 = 0$ . Moreover, it also vanishes in zero field  $H = 0$  due to the rotational symmetry of Eq. (2). It is well known that lamellar structures emerging in an isotropic environment are characterized by particularly soft small-amplitude, i.e., phonon excitations that possess the Landau-Peierls form [8]. In this case the contribution to the energy from the far field of screw dislocations, which can be captured in terms of a static phonon field, vanishes [8–10,67] in agreement with Eq. (6). Technically, this is here due to a cancellation of exchange and DMI energies. The prefactor of the logarithmic contribution in Eq. (6) remains finite however at  $H = 0$  if magnetocrystalline anisotropies are taken into

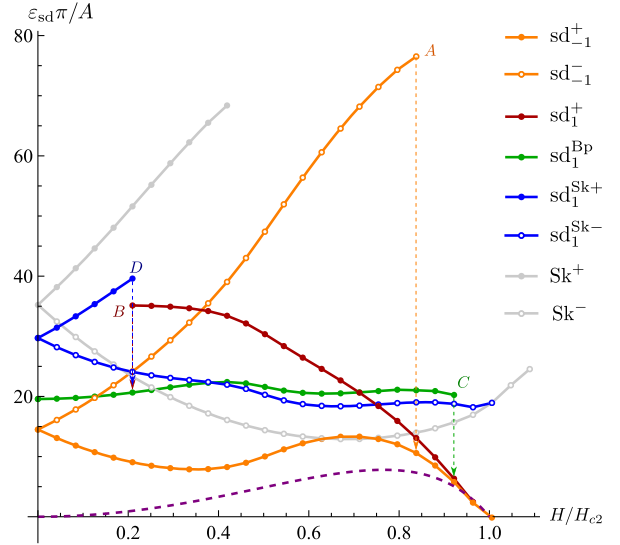


FIG. 3. Energy per length of the various screw dislocation lines shown in Figs. 2 and 4, as a function of  $H$  with a comparison to the skyrmion string energy (gray lines) whose core magnetization is aligned ( $Sk^+$ ) or antialigned ( $Sk^-$ ) with the field. The energies were obtained by micromagnetic simulations for a cylinder-shaped system with radius  $R = 5\lambda_h$ . Dashed line shows the logarithmic contribution of the far field in Eq. (6) assuming  $\rho_{\text{core}} = \lambda_h/2$  for illustration. The energy of dislocations  $sd_{-1}^-$  and  $sd_1^+$  vanishes at  $H_{c2}$  where they can be identified as vortex lines of the  $XY$ -order parameter. The energy of  $sd_1^{\text{Sk}^-}$  merges at  $H_{c2}$  with that of the skyrmion string  $Sk^-$ . Points A–D mark field values where the corresponding configurations became unstable in numerical simulations due to the lattice discreteness.

account that explicitly break the continuous rotational symmetry of the theory [46].

*Core structure of screw dislocations.*—Having established the far field of screw dislocations we now turn to the discussion of their core structures. We employ micromagnetic simulations [46] in order to determine the core and its energy. First, we focus on the case with strength  $\nu = -1$ , see Fig. 2. The magnetization can here be continuously extrapolated from the far field towards the core resulting in a smooth texture. There exist two energetically degenerate configurations at zero field where the core magnetization is either aligned or antialigned with the field, respectively, denoted by  $sd_{-1}^-$  and  $sd_1^+$  in the following. In order to decrease DMI energy, the core deforms elliptically such that it mimics a small Bloch-domain wall with preferred chirality. In addition, we found that close to zero field the ellipse is further deformed into a banana-shape structure, see cross sections in Fig. 2, that leads to a periodicity of the core along the  $z$  axis with an enhanced wavelength  $2\lambda_h$ . For finite field  $H$ , the configuration with the aligned core magnetization  $sd_{-1}^-$  is energetically favored, see Fig. 3. The precise  $H$  dependence of the dislocation energy depends on the system size  $R$  but it vanishes for  $H \rightarrow H_{c2}$ .

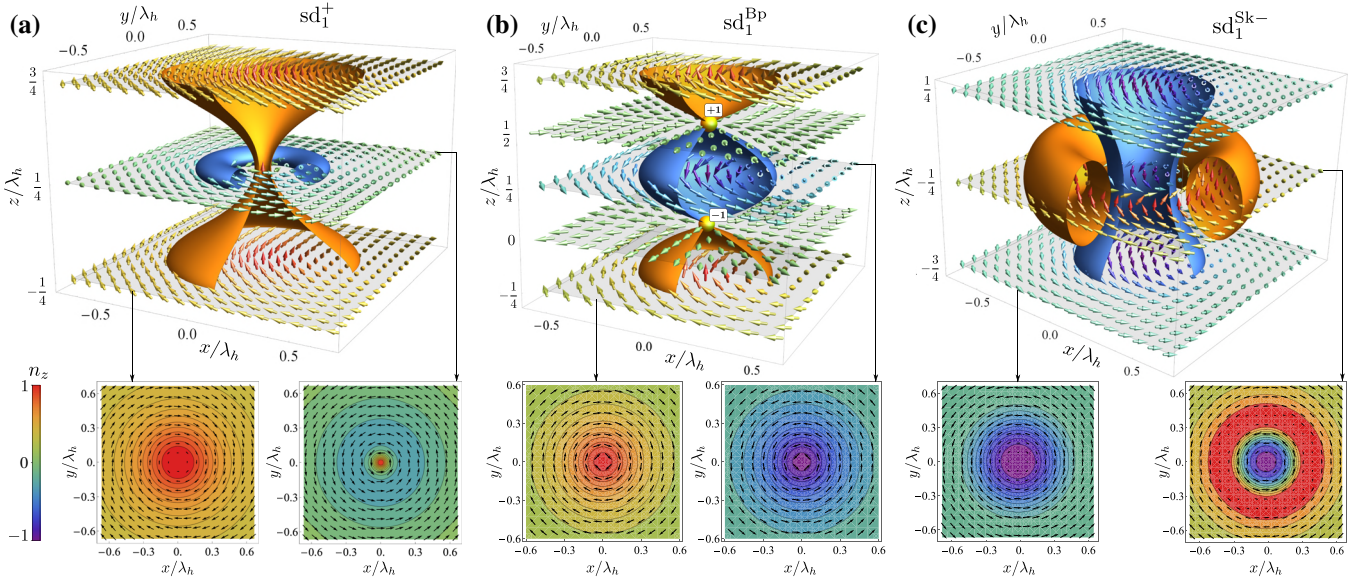


FIG. 4. Core of various screw dislocations with strength  $\nu = 1$  obtained by micromagnetic simulations. Orange and blue isosurfaces are, respectively, defined by  $n_z = 1/2$  and  $n_z = -1/2$  except in panel (a) where  $n_z = 1/2$  and  $n_z = -1/4$ . (a) Dislocation  $sd_1^+$  with core magnetization aligned with the field for  $H = 0.21H_{c2}$ . (b) Dislocation  $sd_1^{\text{Bp}}$  for  $H = 0$  with an alternating core magnetization separated by Bloch points (yellow spheres) with alternating topological charges  $\pm 1$ . (c) Dislocation  $sd_1^{\text{Sk-}}$  at  $H = 0$  with an antialigned core magnetization; it smoothly connects to a skyrmion string configuration for  $H \rightarrow H_{c2}$ .

There exists in fact a screw dislocation for each strength  $\nu$  whose energy vanishes at  $H_{c2}$ . The phase transition at  $H_{c2}$  corresponds to a magnon condensation [68] that is in the  $XY$ -universality class. Employing a standard Holstein-Primakoff expansion around the field-polarized state  $\mathbf{n} = \hat{z} + [\psi e^{-i2\pi z/\lambda_h}(\hat{x} + i\hat{y}) + \text{c.c.}] + \mathcal{O}(|\psi|^2)$  for  $H > 0$  the complex spin wave function  $\psi$  can be identified with the corresponding  $XY$ -order parameter. When it condenses for  $H \lesssim H_{c2}$  with nonzero constant  $\psi$ , long-range conical order emerges. The  $U(1)$  symmetry of the complex wave function  $\psi$  then also supports vortex line solutions given by  $\psi \sim e^{-i\nu z}$  with an amplitude vanishing at the core. The size of the vortex core is determined by the correlation length of the condensate,  $\xi \sim 1/\sqrt{1 - H/H_{c2}}$  [69], and is thus independent of  $z$ . This implies a cylindrical core of the vortex line close to  $H_{c2}$ . Hence, these vortex lines can be identified with a special type of screw dislocations of the helimagnetic order that possess a smooth magnetization at the core that is aligned with the applied field.

Let us consider the corresponding solution with strength  $\nu = 1$  denoted by  $sd_1^+$  in Fig. 4(a). Here, the vortex structure of the  $(x, y)$  components of magnetization in the far field continuously alternate from a divergenceless to a rotationless configuration as a function of  $z$  with a topological charge  $N_{\text{top}} = \frac{1}{2}(1 - H/H_{c2})$  that is independent of  $z$ . It is instructive to focus on the planes  $z = \frac{1}{2}(m \pm \frac{1}{2})\lambda_h$  in Eq. (4) with  $m \in \mathbb{Z}$ , where a divergenceless configuration is realized. As the core is approached, the magnetization smoothly rotates in a right-handed or left-handed manner until it is aligned with the field at the center,

see lower panels in Fig. 4(a). Whereas the former texture is favored by the DMI, the latter is disfavored. As a consequence, the core, that is cylindrical close to  $H_{c2}$ , becomes undulated along the  $z$  axis for smaller fields with a contraction on the  $z$  planes housing the disfavored textures. The energetic cost of the latter also leads to an increase of the dislocation energy for decreasing  $H$ . In the simulations we found that this particular screw dislocation structure cannot be maintained for lowest magnetic fields. Instead, a first order transition to a different structure occurs at point  $B$  in Fig. 3, to which we turn next.

The energy cost of the disfavored configurations shown in the lower right panel of Fig. 4(a) can be avoided by switching the core magnetization within these planes. An alternating core magnetization along the  $z$  axis is indeed characteristic for the screw dislocation  $sd_1^{\text{Bp}}$  shown in Fig. 4(b). At zero field, it realizes a Bloch-like meron structure on the planes  $z = \frac{1}{2}(m \pm \frac{1}{2})\lambda_h$  that are both favored by the DMI. These merons possess alternating skyrmion charges  $N_{\text{top}} = \pm \frac{1}{2}$  that implies the presence of Bloch points with alternating topological charges  $\pm 1$  [70] positioned in the core on the intermediate planes  $z = m\lambda_h/2$  with  $m \in \mathbb{Z}$ . This screw dislocation  $sd_1^{\text{Bp}}$  with a chain of Bloch points at its core is the most stable configuration for  $\nu = 1$  close to zero field but it is energetically more costly than the dislocations  $sd_{\pm 1}^{\pm}$  with  $\nu = -1$ . It can be maintained for a large field range but it becomes unstable in the simulations at point  $C$  in Fig. 3 where oppositely charged Bloch points annihilate before reaching the critical field  $H_{c2}$ .

There exists a third screw dislocation with strength  $\nu = 1$  that again possesses a smooth core texture without singularities. Its core magnetization is either fully aligned or antialigned with the applied field. Both configurations,  $sd_1^{\text{Sk}+}$  and  $sd_1^{\text{Sk}-}$ , respectively, are degenerate at zero field, but the antialigned core is energetically favored at finite  $H$ , see Fig. 3. In the simulations, the configuration with the aligned core can only be stabilized for small field values up to point  $D$ . In order to elucidate the core structure, we focus in Fig. 4(c) on  $sd_1^{\text{Sk}-}$  at  $H = 0$  and consider again the planes  $z = \frac{1}{2}(m \pm \frac{1}{2})\lambda_h$  with a divergenceless configuration of the magnetization in the far field. As the core is approached within these planes, the magnetization smoothly rotates in a Bloch-like fashion that is favored by the DMI. In half of these planes it is sufficient to rotate the magnetization by  $\pi/2$  but in the complementary planes a rotation by  $3\pi/2$  is required in order to reach a uniformly magnetized core. The topological charge within each plane is given by  $N_{\text{top}} = -\frac{1}{2}(1 + H/H_{c2})$ . As the field increases, the in-plane texture transforms from a meron with  $N_{\text{top}} = -\frac{1}{2}$  to a skyrmion with  $N_{\text{top}} = -1$ . In fact, as the critical field  $H_{c2}$  is approached this screw dislocation smoothly converts into a skyrmion configuration of the field-polarized state. The screw dislocation  $sd_1^{\text{Sk}}$  close to  $H_{c2}$  can thus be viewed as a bound state of a skyrmion string with a vortex of the  $XY$ -order parameter  $\psi$ .

*Outlook.*—While we focused here on the most relevant screw dislocations with smallest Burgers vector, i.e.,  $|\nu| = 1$ , the micromagnetic core structure for higher strength  $|\nu|$  can be even richer, as will be shown elsewhere. A number of techniques were recently developed that might enable the experimental identification of screw dislocations, including scalar [71] and vector [72,73] x-ray tomography, as well as holographic vector field electron tomography [74]. Screw dislocations are known to proliferate and form regular arrays at twist grain boundaries [8,29]. Interestingly, a multidomain state with twist grain boundaries is naturally expected to occur in the cubic chiral magnets after zero-field cooling [1,4,30], and, consequently, this state is an ideal candidate for experimentally spotting helimagnetic screw dislocations.

M. A. acknowledges useful discussions with Josse Muller. This work is supported by the Deutsche Forschungsgemeinschaft (DFG, German Research Foundation) in the framework of SFB 1143 (project A07; project-id 247310070), TRR 288-422213477 (project A11), project-id 270344603, and SPP 2137 (project-id 324327023). In part, this work was supported by the Program of Fundamental Research of the Department of Physics and Astronomy of the National Academy of Sciences of Ukraine (Project No. 0120U100855).

- [1] P. Bak and M. H. Jensen, *J. Phys. C* **13**, L881 (1980).  
 [2] O. Nakanishi, A. Yanase, A. Hasegawa, and M. Kataoka, *Solid State Commun.* **35**, 995 (1980).

- [3] Y. Ishikawa, K. Tajima, D. Bloch, and M. Roth, *Solid State Commun.* **19**, 525 (1976).  
 [4] B. Lebech, J. Bernhard, and T. Freltoft, *J. Phys. Condens. Matter* **1**, 6105 (1989).  
 [5] M. Uchida, Y. Onose, Y. Matsui, and Y. Tokura, *Science* **311**, 359 (2006).  
 [6] T. Adams, A. Chacon, M. Wagner, A. Bauer, G. Brandl, B. Pedersen, H. Berger, P. Lemmens, and C. Pfleiderer, *Phys. Rev. Lett.* **108**, 237204 (2012).  
 [7] S. Seki, X. Z. Yu, S. Ishiwata, and Y. Tokura, *Science* **336**, 198 (2012).  
 [8] P. M. Chaikin and T. C. Lubensky, *Principles of Condensed Matter Physics*, 1st ed. (Cambridge University Press, Cambridge, England, 2000).  
 [9] P. G. de Gennes and J. Prost, *The Physics of Liquid Crystals* (Oxford University Press, Cambridge, England, 1995).  
 [10] *Soft Matter Physics: An Introduction*, edited by M. Kleman and O. D. Lavrentovich (Springer, New York, 2004).  
 [11] M. Janoschek, M. Garst, A. Bauer, P. Krautscheid, R. Georgii, P. Böni, and C. Pfleiderer, *Phys. Rev. B* **87**, 134407 (2013).  
 [12] S. Buhandt and L. Fritz, *Phys. Rev. B* **88**, 195137 (2013).  
 [13] I. Živković, J. S. White, H. M. Rønnow, K. Prša, and H. Berger, *Phys. Rev. B* **89**, 060401(R) (2014).  
 [14] S. A. Brazovskii, I. E. Dzyaloshinskii, and A. R. Muratov, *Sov. Phys. JETP* **66**, 625 (1987), <http://www.jetp.ras.ru/cgi-bin/e/index/e/66/3/p625?a=list>.  
 [15] J. Kindervater, I. Stasinopoulos, A. Bauer, F. X. Haslbeck, F. Rucker, A. Chacon, S. Mühlbauer, C. Franz, M. Garst, D. Grundler, and C. Pfleiderer, *Phys. Rev. X* **9**, 041059 (2019).  
 [16] C. Pfleiderer, S. R. Julian, and G. G. Lonzarich, *Nature (London)* **414**, 427 (2001).  
 [17] C. Pfleiderer, P. Boni, T. Keller, U. K. Rossler, and A. Rosch, *Science* **316**, 1871 (2007).  
 [18] P. Pedrazzini, H. Wilhelm, D. Jaccard, T. Jarlborg, M. Schmidt, M. Hanfland, L. Akselrud, H. Q. Yuan, U. Schwarz, Y. Grin, and F. Steglich, *Phys. Rev. Lett.* **98**, 047204 (2007).  
 [19] R. Ritz, M. Halder, M. Wagner, C. Franz, A. Bauer, and C. Pfleiderer, *Nature (London)* **497**, 231 (2013).  
 [20] J. Schmalian and M. Turlakov, *Phys. Rev. Lett.* **93**, 036405 (2004).  
 [21] J. Toner, *Phys. Rev. B* **26**, 462 (1982).  
 [22] G. Grinstein, T. C. Lubensky, and J. Toner, *Phys. Rev. B* **33**, 3306 (1986).  
 [23] Z. Zhai and L. Radzihovsky, *Ann. Phys. (Amsterdam)* **435**, 168509 (2021).  
 [24] M. Kléman, *Philos. Mag.* **22**, 739 (1970).  
 [25] F. Li, T. Nattermann, and V. L. Pokrovsky, *Phys. Rev. Lett.* **108**, 107203 (2012).  
 [26] T. Nattermann and V. L. Pokrovsky, *J. Exp. Theor. Phys.* **127**, 922 (2018).  
 [27] P. Schoenherr, J. Müller, L. Köhler, A. Rosch, N. Kanazawa, Y. Tokura, M. Garst, and D. Meier, *Nat. Phys.* **14**, 465 (2018).  
 [28] Y. Bouligand, *Dislocations in Solids* (North-Holland Publishing Company, New York, 1983), Chap. 23.  
 [29] N. Martin, M. Deutsch, G. Chaboussant, F. Damay, P. Bonville, L. N. Fomicheva, A. V. Tsvyashchenko, U. K. Rössler, and I. Mirebeau, *Phys. Rev. B* **96**, 020413(R) (2017).

- [30] A. Bauer, A. Chacon, M. Wagner, M. Halder, R. Georgii, A. Rosch, C. Pfeleiderer, and M. Garst, *Phys. Rev. B* **95**, 024429 (2017).
- [31] P. Milde, L. Köhler, E. Neuber, P. Ritzinger, M. Garst, A. Bauer, C. Pfeleiderer, H. Berger, and L. M. Eng, *Phys. Rev. B* **102**, 024426 (2020).
- [32] A. Dussaux, P. Schoenherr, K. Koumpouras, J. Chico, K. Chang, L. Lorenzelli, N. Kanazawa, Y. Tokura, M. Garst, A. Bergman, C. L. Degen, and D. Meier, *Nat. Commun.* **7**, 12430 (2016).
- [33] P. Schoenherr, M. Stepanova, E. N. Lysne, N. Kanazawa, Y. Tokura, A. Bergman, and D. Meier, [arXiv:2105.00658](https://arxiv.org/abs/2105.00658).
- [34] A. Bogdanov and A. Hubert, *J. Magn. Magn. Mater.* **138**, 255 (1994).
- [35] S. Mühlbauer, B. Binz, F. Jonietz, C. Pfeleiderer, A. Rosch, A. Neubauer, R. Georgii, and P. Böni, *Science* **323**, 915 (2009).
- [36] X. Z. Yu, Y. Onose, N. Kanazawa, J. H. Park, J. H. Han, Y. Matsui, N. Nagaosa, and Y. Tokura, *Nature (London)* **465**, 901 (2010).
- [37] C. Back, V. Cros, H. Ebert, K. Everschor-Sitte, A. Fert, M. Garst, T. Ma, S. Mankovsky, T. L. Monchesky, M. Mostovoy, N. Nagaosa, S. S. P. Parkin, C. Pfeleiderer, N. Reyren, A. Rosch, Y. Taguchi, Y. Tokura, K. von Bergmann, and J. Zang, *J. Phys. D* **53**, 363001 (2020).
- [38] A. O. Leonov, T. L. Monchesky, J. C. Loudon, and A. N. Bogdanov, *J. Phys. Condens. Matter* **28**, 35LT01 (2016).
- [39] F. N. Rybakov, A. B. Borisov, S. Blügel, and N. S. Kiselev, *Phys. Rev. Lett.* **115**, 117201 (2015).
- [40] H. Du, X. Zhao, F. N. Rybakov, A. B. Borisov, S. Wang, J. Tang, C. Jin, C. Wang, W. Wei, N. S. Kiselev, Y. Zhang, R. Che, S. Blügel, and M. Tian, *Phys. Rev. Lett.* **120**, 197203 (2018).
- [41] H. R. O. Sohn, S. M. Vlasov, V. M. Uzdin, A. O. Leonov, and I. I. Smalyukh, *Phys. Rev. B* **100**, 104401 (2019).
- [42] A. O. Leonov, C. Pappas, and I. I. Smalyukh, *Phys. Rev. B* **104**, 064432 (2021).
- [43] G. P. Müller, F. N. Rybakov, H. Jónsson, S. Blügel, and N. S. Kiselev, *Phys. Rev. B* **101**, 184405 (2020).
- [44] R. Voinescu, J.-S. B. Tai, and I. I. Smalyukh, *Phys. Rev. Lett.* **125**, 057201 (2020).
- [45] The displacement field  $\mathbf{u}$  describes small deviations of the fronts of constant phases  $\phi(\mathbf{r}) = \text{const}$  of the helimagnetic order where  $\phi(\mathbf{r}) = 2\pi(\mathbf{r} + \mathbf{u})\hat{z}/\lambda_h$ .
- [46] See Supplemental Material at <http://link.aps.org/supplemental/10.1103/PhysRevLett.128.157204>, which includes Refs. [42,47–66], for detailed discussion of the micromagnetic simulations, derivation of the far field of the screw dislocations, effect of anisotropy, and further details of the core structure.
- [47] A. Vansteenkiste, J. Leliaert, M. Dvornik, M. Helsen, F. Garcia-Sanchez, and B. Van Waeyenberge, *AIP Adv.* **4**, 107133 (2014).
- [48] The Object Oriented MicroMagnetic Framework, developed by M. J. Donahue and D. Porter mainly, from NIST. We used the 3D version of the 1.2b3 release.
- [49] D. Cortés-Ortuño, M. Beg, V. Nehruji, R. A. Pepper, and H. Fangohr, OOMMF extension: Dzyaloshinskii-Moriya interaction (DMI) for crystallographic classes T and O (2018).
- [50] E. A. Karhu, U. K. Röbler, A. N. Bogdanov, S. Kahwaji, B. J. Kirby, H. Fritzsche, M. D. Robertson, C. F. Majkrzak, and T. L. Monchesky, *Phys. Rev. B* **85**, 094429 (2012).
- [51] M. N. Wilson, E. A. Karhu, D. P. Lake, A. S. Quigley, S. Meynell, A. N. Bogdanov, H. Fritzsche, U. K. Röbler, and T. L. Monchesky, *Phys. Rev. B* **88**, 214420 (2013).
- [52] S. Rohart and A. Thiaville, *Phys. Rev. B* **88**, 184422 (2013).
- [53] M. N. Wilson, A. B. Butenko, A. N. Bogdanov, and T. L. Monchesky, *Phys. Rev. B* **89**, 094411 (2014).
- [54] I. E. Dzyaloshinskii and B. A. Ivanov, *JETP Lett.* **29**, 540 (1979), [http://jetpletters.ru/ps/1455/article\\_22156.pdf](http://jetpletters.ru/ps/1455/article_22156.pdf).
- [55] A. M. Kosevich, B. A. Ivanov, and A. S. Kovalev, *Phys. Rep.* **194**, 117 (1990).
- [56] P. J. Ackerman and I. I. Smalyukh, *Phys. Rev. X* **7**, 011006 (2017).
- [57] Jung-Shen B. Tai and I. I. Smalyukh, *Phys. Rev. Lett.* **121**, 187201 (2018).
- [58] P. Sutcliffe, *J. Phys. A* **51**, 375401 (2018).
- [59] H. Hopf, *Math. Ann.* **104**, 637 (1931).
- [60] V. Kravchuk and D. Sheka, *Phys. Solid State* **49**, 1923 (2007).
- [61] A. P. Malozemoff and J. C. Slonzewski, *Magnetic Domain Walls in Bubble Materials* (Academic Press, New York, 1979).
- [62] W. Döring, *J. Appl. Phys.* **39**, 1006 (1968).
- [63] O. V. Pylypovskyi, D. D. Sheka, and Y. Gaididei, *Phys. Rev. B* **85**, 224401 (2012).
- [64] M. Charilaou, *Phys. Rev. B* **102**, 014430 (2020).
- [65] Y. Li, L. Pierobon, M. Charilaou, H.-B. Braun, N. R. Walet, J. F. Löffler, J. J. Miles, and C. Moutafis, *Phys. Rev. Research* **2**, 033006 (2020).
- [66] K. Shimizu, S. Okumura, Y. Kato, and Y. Motome, *Phys. Rev. B* **103**, 184421 (2021).
- [67] C. D. Santangelo, *Liquid Crystals Today* **15**, 11 (2006).
- [68] T. Giamarchi, C. Rüegg, and O. Tchernyshyov, *Nat. Phys.* **4**, 198 (2008).
- [69] B. A. Ivanov and D. D. Sheka, *Low Temp. Phys.* **21**, 881 (1995), [https://ritm.knu.ua/downloads/pub/Ivanov\\_LTP.95.pdf](https://ritm.knu.ua/downloads/pub/Ivanov_LTP.95.pdf).
- [70] The topological charge  $c$  of a Bloch point is defined by  $c = \int_V d\mathbf{r} \nabla \cdot \mathbf{\Omega}$ , where  $V$  is a small volume around the Bloch point and  $\mathbf{\Omega}_i = \epsilon_{ijk}(1/8\pi)\mathbf{n}(\partial_j \mathbf{n} \times \partial_k \mathbf{n})$ .
- [71] S. Seki, M. Suzuki, M. Ishibashi, R. Takagi, N. D. Khanh, Y. Shiota, K. Shibata, W. Koshibae, Y. Tokura, and T. Ono, *Nat. Mater.* **21**, 181 (2022).
- [72] C. Donnelly, M. Guizar-Sicairos, V. Scagnoli, S. Gliga, M. Holler, J. Raabe, and L. J. Heyderman, *Nature (London)* **547**, 328 (2017).
- [73] C. Donnelly, K. L. Metlov, V. Scagnoli, M. Guizar-Sicairos, M. Holler, N. S. Bingham, J. Raabe, L. J. Heyderman, N. R. Cooper, and S. Gliga, *Nat. Phys.* **17**, 316 (2021).
- [74] D. Wolf, N. Biziere, S. Sturm, D. Reyes, T. Wade, T. Niermann, J. Krehl, B. Warot-Fonrose, B. Büchner, E. Snoeck, C. Gatel, and A. Lubk, *Commun. Phys.* **2**, 87 (2019).